*American Mineralogist, Volume 60, pages 188–199, 1975*

# Synthesis and Solid Solubility of Trioctahedral Brittle Micas in the System $CaO–MgO–Al_2O_3–SiO_2–H_2O$

MARTIN OLESCH

*Mineralogisches Institut der Universität Kiel,*
*2300 Kiel, Olshausenstrasse 40/60, Germany*

**Abstract**

Single-phase trioctahedral brittle micas (clintonite, xanthophyllite, brandisite) of compositions $Ca(Mg_{1+z}Al_{2-z})(Al_{4-z}Si_zO_{10})(OH)_2$ with $z$ from 0.6 to 1.4 were synthesized on the join $CaO:3MgO:Al_2O_3:2SiO_2 + xH_2O–CaO:MgO:3Al_2O_3 + xH_2O$ (substitution $Al^{IV} + Al^{VI} = MgSi$) at 600–870° at 2 kbar water pressure. The Ca analog of phlogopite, *i.e.*, $CaMg_3(Al_2Si_2O_{10})(OH)_2$ could not be synthesized. Solid solubility of the trioctahedral towards dioctahedral calcium micas (*e.g.*, margarite) was studied on two joins starting with $z = 1.17$ and $z = 1.0$. These two joins involve the compositions $Ca(Mg_{4.5-2z}Al_{z-0.33})(Al_{4-z}Si_zO_{10})(OH)_2$ and $Ca(Mg_{4-2z}Al_z)(Al_{4-z}Si_zO_{10})(OH)_2$ (substitution $2Mg + Al^{IV} = Al^{VI} + Si$), respectively. Maximum solid solubility towards the dioctahedral component on these joins was found to be 10 mole percent ($1.17 < z < 1.27$) and 24 mole percent ($1.0 < z < 1.24$), respectively.

All micas synthesized were of the 1 *M* (or 3 *T*) polymorphic type. Their lattice constants *a, b, c, V* decrease with decreasing $z$ in the strictly trioctahedral micas and also with increasing dioctahedral component. $\beta$ remains constant. The solid solubility encompasses and, on the alumina-rich side, even exceeds the variation in natural calcium micas.

## Introduction

The composition of trioctahedral brittle micas can be represented by the simplified general formula

$$Ca(Mg,Fe^{2+},Fe^{3+},Al)_3(Al,Si)_4O_{10}(OH,F,O)_2.$$

Although not very common, they are of general mineralogical and petrological interest because they occur in thermally metamorphosed calcium- and aluminum-rich rocks. What makes this group intriguing from the view of crystal chemistry is their high proportion of aluminum in tetrahedral sites. Some rare mineral species such as bityite (≈ bowleite), anandite, and ephesite are structurally related to the trioctahedral brittle micas, but incorporate larger amounts of cations such as Li, Be, Ba, Na, and $Fe^{2+}$ so as to be chemically distinct from xanthophyllite, clintonite, and brandisite, the more common rock-forming trioctahedral calcium micas. A survey of the reported analyses for brittle micas showed that the cations Ca, Mg, Al, and Si are predominant, iron oxide (total iron) amounting to at most 3.5 wt percent, $Na_2O$ to at most 1.9 wt percent, and all other oxides being less than 0.7 wt percent. The chemical composition of trioctahedral calcium micas can thus be closely represented in the system $CaO–MgO–Al_2O_3–SiO_2–H_2O$.

From the many names of so-called varieties of trioctahedral calcium micas (Hintze, 1897) the terms brandisite, clintonite (seybertite), and xanthophyllite have been widely used. However, Tschermak and Sipöcz (1879) pointed out that the name clintonite should be used exclusively, because the variability in chemical composition and physical properties within this group is very small and does not warrant distinction of several mineral species. This latter statement has been supported by further chemical (Koch, 1935) and structural (Forman *et al*, 1967a,b) investigations. For a thorough discussion of nomenclature of trioctahedral calcium micas the interested reader is referred to the compilation in Olesch (1973). In the present paper the name clintonite will be used exclusively for the entire group of trioctahedral calcium micas represented by the above general formula.

Previous syntheses of trioctahedral calcium micas have been mentioned by Roy and Tuttle (1961; unpublished results of De Vries and Roy, 1954) and Christophe-Michel-Lévy (1964). Some data on solid solubility are given by Velde (1973). The present paper reports the results of synthesis experiments as a function of temperature, water pressure, and bulk composition. The data were used to determine the limits of solid solubility and some physical properties of the mica phases.

## Experimental Methods

### *High Pressure-High Temperature Apparatus*

Synthesis runs were performed in cold seal autoclaves and in an internally-heated gas apparatus. The cold-seal pressure vessels were similar in design and dimensions to those described by Luth and Tuttle (1963). Water pressure was continuously monitored by Bourdon gauges, and the precision of the pressures reported is ±5 percent at pressures of 2 kbar and below, and ±2 percent at higher pressures. Temperatures were controlled and measured through chromel-alumel thermocouples calibrated against the melting points of NaCl (800.5°C) and zinc (419.5°C). To avoid error by contamination and/or recrystallization, the thermocouples were changed after every run above 700°C. Considering all errors, the precision of the temperatures reported is ±5°C. Runs at *P-T* conditions above 800°C at 2 kbar and above 700°C at 5 kbar were performed in an internally-heated gas apparatus as described by Seifert (1970) with uncertainties in pressure of ±2 percent and in temperature of ±10°C. The pressure effect on the emf of the Pt-Pt90Rh10 thermocouples has been neglected.

### *Starting Materials*

For most of the compositions investigated, dehydrated gels were prepared according to the method described by Hamilton and Henderson (1968). Checking the chemical composition of some gels by chemical analysis yielded good agreement of intended and determined stoichiometric ratios. However, up to 2.38 wt percent $CO_2$ were found in the gels (*cf* Ito and Arem, 1970). This is not surprising, because some water is always retained in gels, and moist finely divided Ca-bearing gels can be expected to pick up $CO_2$ rapidly from the air, due to their strongly basic reaction. Considering the amounts of gel and water used in the experiments, this $CO_2$ content corresponds to an $X_{CO_2}$ up to 2.2 mole percent in the gas phase. The effect on the products of synthesis of this $CO_2$ content in the starting material will be discussed below. Only for some compositions within the field of solid solubility of the mica phase have mixtures of gels been employed (see Table 1, section A). Although the gels used in preparing gel mixtures were carefully dried for several hours at 850°C, the chemical composition of these mixtures is less well defined because of the still varying amounts of adsorbed water.

The gels were found to be optically isotropic and amorphous to X-rays. For the runs, some 25 to 35 mg of gel and 5 to 10 mg of doubly distilled water were welded into gold or platinum tubes, the weights being checked after every step of preparation and after the runs, and only tight tubes being considered.

TABLE 1. Composition of Gels and Gel Mixtures and Corresponding Theoretical Structural Formula of Micas

| # | Oxide Proportions | | | | Theoretical Mica Formula on the Basis of 22 Cation Valencies (Cations only) | | | | |
|---|---|---|---|---|---|---|---|---|---|
| | CaO | MgO | $Al_2O_3$ | $SiO_2$ | Ca | $Mg^{VI}$ | $Al^{VI}$ | $Al^{IV}$ | $Si^{IV}$ |
| **Section A** | | | | | | | | | |
| 1* | 1 | 3.0 | 1.0 | 2.0 | 1 | 3.0 | - | 2.0 | 2.0 |
| 2 | 1 | 2.75 | 1.25 | 1.75 | 1 | 2.75 | 0.25 | 2.25 | 1.75 |
| 4 | 1 | 2.5 | 1.5 | 1.5 | 1 | 2.5 | 0.5 | 2.5 | 1.5 |
| C | 1 | 2.38 | 1.62 | 1.38 | 1 | 2.38 | 0.62 | 2.62 | 1.38 |
| B | 1 | 2.33 | 1.67 | 1.33 | 1 | 2.33 | 0.67 | 2.67 | 1.33 |
| A | 1 | 2.29 | 1.71 | 1.29 | 1 | 2.29 | 0.71 | 2.71 | 1.29 |
| 5 | 1 | 2.25 | 1.75 | 1.25 | 1 | 2.25 | 0.75 | 2.75 | 1.25 |
| D | 1 | 2.17 | 1.83 | 1.17 | 1 | 2.17 | 0.83 | 2.83 | 1.17 |
| E | 1 | 2.1 | 1.9 | 1.1 | 1 | 2.1 | 0.9 | 2.9 | 1.1 |
| 6 | 1 | 2.0 | 2.0 | 1.0 | 1 | 2.0 | 1.0 | 3.0 | 1.0 |
| F | 1 | 1.9 | 2.1 | 0.9 | 1 | 1.9 | 1.1 | 3.1 | 0.9 |
| 7 | 1 | 1.75 | 2.25 | 0.75 | 1 | 1.75 | 1.25 | 3.25 | 0.75 |
| G | 1 | 1.6 | 2.4 | 0.6 | 1 | 1.6 | 1.4 | 3.4 | 0.6 |
| 8 | 1 | 1.5 | 2.5 | 0.5 | 1 | 1.5 | 1.5 | 3.5 | 0.5 |
| 18 | 1 | 1.25 | 2.75 | 0.25 | 1 | 1.25 | 1.75 | 3.75 | 0.25 |
| **Section B** | | | | | | | | | |
| 9 | 1 | 1.83 | 1.83 | 1.33 | 1 | 1.83 | 1.0 | 2.67 | 1.33 |
| 35 | 1 | 1.92 | 1.83 | 1.29 | 1 | 1.92 | 0.96 | 2.71 | 1.29 |
| 10 | 1 | 2.0 | 1.83 | 1.25 | 1 | 2.0 | 0.92 | 2.75 | 1.25 |
| 34 | 1 | 2.08 | 1.83 | 1.21 | 1 | 2.08 | 0.88 | 2.79 | 1.21 |
| **Section C** | | | | | | | | | |
| 27 | 1 | 1.0 | 2.0 | 1.5 | 1 | 1.0 | 1.5 | 2.5 | 1.5 |
| 28 | 1 | 1.2 | 2.0 | 1.4 | 1 | 1.2 | 1.4 | 2.6 | 1.4 |
| 29 | 1 | 1.4 | 2.0 | 1.3 | 1 | 1.4 | 1.3 | 2.7 | 1.3 |
| 30 | 1 | 1.6 | 2.0 | 1.2 | 1 | 1.6 | 1.2 | 2.8 | 1.2 |
| 32 | 1 | 1.7 | 2.0 | 1.15 | 1 | 1.7 | 1.15 | 2.85 | 1.15 |
| 31 | 1 | 1.8 | 2.0 | 1.1 | 1 | 1.8 | 1.1 | 2.9 | 1.1 |
| 33 | 1 | 1.9 | 2.0 | 1.05 | 1 | 1.9 | 1.05 | 2.95 | 1.05 |

* Numbers designate compositions prepared directly as a gel, whereas letters represent gel mixtures (cf. text).

### *Identification of Phases*

The run products were investigated with binocular and petrographic microscopes, and by X-ray powder diffractometry. The color of the products was generally white as to be expected from the components used. Only in very long runs (of more than 2000 hours duration) at temperatures below 420°C were some products lightly gray. No additional phases could, however, be identified microscopically or by X-rays. It is tentatively concluded that the $CO_2$ present in the charge (see above) was reduced to carbon by hydrogen that, being generated by reaction of the hydrous pressure medium with the bomb walls, diffused slowly into the capsules. Assuming oxygen fugacities close to the Ni–NiO buffer (Huebner, 1971), graphite is stable in a C-H-O atmosphere

below 470°C at 2 kbar and 400°C at 1 kbar (French and Eugster, 1965).

Because of the fine-grained nature of most run products, the phases were identified mainly by X-ray powder methods, using a diffractometer with Ni-filtered Cu radiation and a scanning speed of 1° $2\theta$ per minute. Lattice constants were determined from diagrams obtained with 0.25 or 0.125° $2\theta$ per minute scan speed, oscillating several times. Silicon (99.999 Si, Schuchardt, München, Lot No. Si 173) served as an internal standard employing the following peak positions (from Philips Laboratory Service Manual): *111*, 28.466° $2\theta$ Cu$K\alpha$; *220*, 47.302° $2\theta$ Cu$K\alpha$; and *311*, 56.122° $2\theta$ Cu$K\alpha_1$. Reflections below 45° $2\theta$ were evaluated from the Cu$K\alpha$ peaks, those at higher $2\theta$ from Cu$K\alpha_1$. Due to the platy habit of the micas some degree of preferred orientation might be expected, affecting the relative intensities. However, admixture of cork powder or treatment of the sample surface according to Peters (1970) did not affect the intensities significantly. No special precautions were, therefore, taken in the preparation of X-ray samples. Lattice constants were calculated by the least-squares technique using the program of Burnham (1962).

## Chemistry of Natural Trioctahedral Calcium Micas

All chemical analyses reported for these micas were evaluated critically in order to obtain a guide-line for the study in the synthetic system. Analyses made before the important paper by Tschermak and Sipöcz (1879) have not been considered (*cf* Doelter, 1917). Similarly analyses were discarded, where only structural formulae have been reported (Takeuchi and Sadanaga, 1959; Akhundov, Mamedov, and Belov, 1961; Stevenson and Beck, 1965). In the remaining analyses the sum of $SiO_2$ + $Al_2O_3$ + MgO + CaO + $H_2O$ amounts to between 94.55 and 99.9 wt percent, justifying the use of these components as a suitable model system. The remaining 0.1 to 5.45 wt percent are represented by (maximum values in wt percent): 0.58 $TiO_2$, 3.24 $Fe_2O_3$, 2.56 FeO, 0.03 MnO, 0.14 SrO, 0.04 BaO, 1.86 $Na_2O$, 0.58 $K_2O$, 1.91 F, 0.25 Cl, (*cf* analyses mentioned in legend to Figure 1).

The analyses were recalculated to mineral formulae on the basis of 22 cation valences (Stevens, 1947). Ca, Ba, Sr, K, Na were assigned to interlayer sites; Si and part of Al were used to fill the tetrahedral positions; and all other atoms including the rest of Al were incorporated in the octahedral positions. Figure 1 shows a plot in a projection of the system CaO(+ SrO + BaO + $Na_2O$ + $K_2O$) − MgO (+ FeO + MnO)

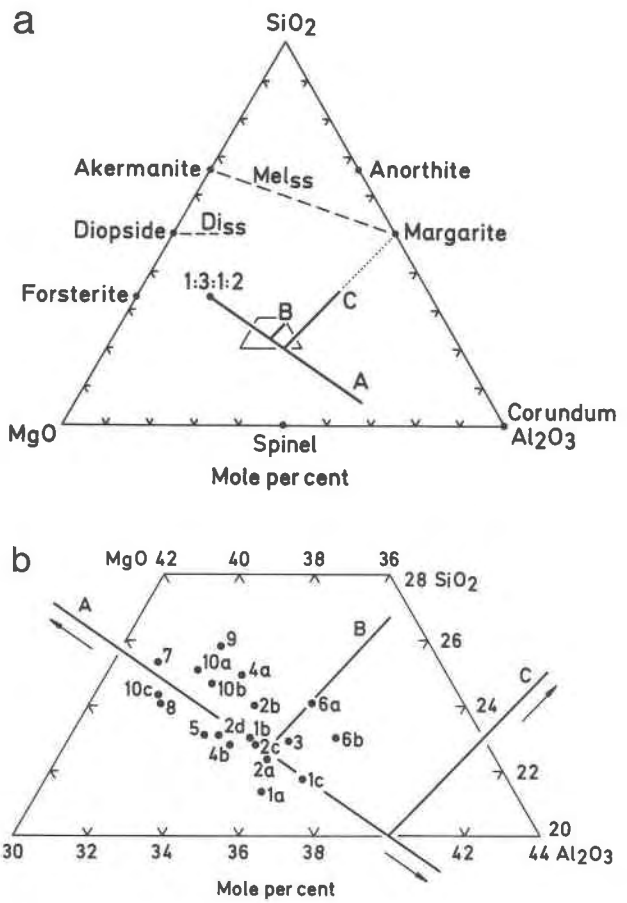


FIG. 1. Analyzed compositions of natural trioctahedral micas, projected in the model system CaO–MgO–$Al_2O_3$–$SiO_2$–$H_2O$ through the CaO and $H_2O$ poles. **a**. The model system with the sections A, B, and C investigated as well as some important mineral phases. The melilite solid solution ($Mel_{ss}$) extends from akermanite to gehlenite, that of diopside ($Di_{ss}$) from pure diopside towards calcium Tschermaks molecule. In this projection both gehlenite and calcium Tschermaks molecule plot at the same composition as margarite and are, therefore, not indicated. The point labelled 1:3:1:2 (molecular proportions CaO:MgO:$Al_2O_3$:$SiO_2$) represents the calcium analog of phlogopite.

**b**. Enlarged portion of the projection. Here, the MgO-component includes the oxides MgO, FeO, and MnO; the $Al_2O_3$-component $Al_2O_3$, $Fe_2O_3$, and $TiO_2$; the $SiO_2$ component only $SiO_2$, and the CaO component CaO, SrO, BaO, $Na_2O$, and $K_2O$.

Locations and references of analyses: **1a** Schischimskaja Gora, Slatoust, Ural (Nikolajew, 1884). **1b** *ibid* (Koch, 1935). **1c** *ibid* (Forman *et al*, 1967a). **2a** Nikolaje-Maximilianowsk, Achmatowsk, Ural (Nikolajew, 1883). **2b** *ibid* (Doelter, 1917; anal. R. Schlaepfer, 1889). **2c** *ibid* (Clarke and Schneider, 1892). **2d** *ibid* (Koch, 1935). **3** Crestmore, California (Eakle, 1916). **4a**, **4b** Monte Costone, Adamello, Alps (Bianchi and Hieke, 1946). **5** Lago della Vacca, Adamello, Alps (Sanero, 1940). **6a**, **6b** Chichibu Mine, Japan (Harada, Kodama, and Sudo, 1965). **7** Amity, New York (Tschermak and Sipöcz, 1879). **8** Pargas, Finland (Laitakari, 1921). **9** Montezuma Valley, California (Forman *et al*, 1967b). **10a** Toal de la Foja, Monzoni, Alps (Tschermak and Sipöcz, 1879). **10b**, **10c** *ibid* (Koch, 1935).

$- Al_2O_3 (+ Fe_2O_3 + TiO_2) - SiO_2 - H_2O$ from the CaO and $H_2O$ poles. The scatter of mica compositions in the projection of Figure 1 might be explained by applying crystal chemical relationships known from the trioctahedral potassium micas (*e.g.*, phlogopite) where the amounts of silica, alumina, and divalent atoms (mainly Mg and $Fe^{2+}$) vary because of the (limited) substitutions $Al^{VI} + Al^{IV} = MgSi$ (phlogopite-eastonite) and $2Al^{VI} = 3\ Mg^{VI}$ (phlogopite-muscovite) (Crowley and Roy, 1964). Whereas, by the first-mentioned substitution, the total number of atoms per formula unit remains constant, the latter implies formation of vacancies in the octahedral layer, *i.e.*, solid solubility towards dioctahedral micas. Starting from a Ca analog of phlogopite, $CaMg_3(Al_2Si_2O_{10})(OH)_2$, the substitution 2 Al → MgSi could lead theoretically to a trioctahedral end member, $Ca(MgAl_2)(Al)_4O_{10}(OH)_2$, whereas the substitution 2 Al → 3 Mg could lead to margarite, $CaAl_2(Al_2Si_2O_{10})(OH)_2$, which is dioctahedral. Line A (Fig. 1) represents compositional variations due to the first-mentioned substitution, which explains most of the variation observed. Solid solubility towards dioctahedral calcium mica, as evidenced by deviations from line A, is more limited. Although some analyses plot slightly below line A, the larger deviations are observed on the $SiO_2$ and $Al_2O_3$ rich side of line A, *i.e.*, in the direction towards margarite (see also Fig. 2). Thus, some linear combination of 2 Al = MgSi and 3 Mg = 2 Al must occur in some natural clintonites, *e.g.*, $2Mg^{VI} + Al^{IV} = Si^{IV} + Al^{VI}$, plotted as B and C in Figure 1. These two lines start from different compositions on join A. These relationships are further emphasized when the

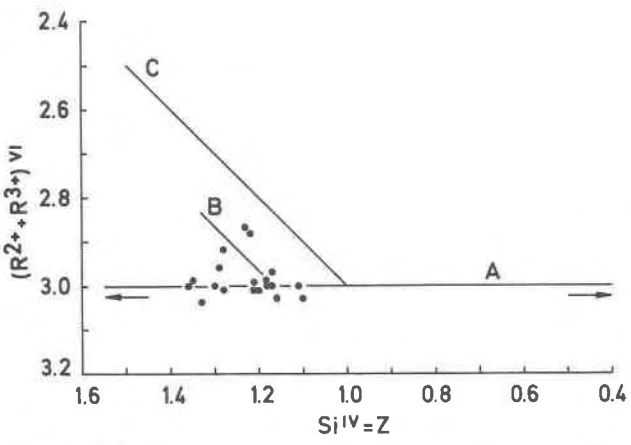


FIG. 2. Plot of tetrahedral *vs* octahedral cations in natural clintonites. A, B, and C are the substitution lines investigated.

TABLE 2. Results of Critical Synthesis Runs on Section A

| Composition* | Run No.** | T (°C) | $P_{H_2O}$ (Kbar) | Duration (Hours) | Condensed Phases Observed*** |
|---|---|---|---|---|---|
| 1 | 78 | 620 | 2.0 | 834 | $Clin_{ss}$,$Chl_{ss}$,Fo,Cc,(Mo) |
| | 63 | 725 | 2.0 | 240 | $Clin_{ss}$,Fo,$Di_{ss}$,(Mo) |
| | 334 | 875 | 2.0 | 121 | $Clin_{ss}$,Fo,$Di_{ss}$,(Mo) |
| | 348 | 925 | 2.0 | 67 | ($Clin_{ss}$,Fo,$Di_{ss}$,Sp,Mo) |
| 2 | 387 | 865 | 2.0 | 240 | $Clin_{ss}$,$Di_{ss}$,Fo,?Sp |
| | 410 | 890 | 2.0 | 214 | $Clin_{ss}$,$Di_{ss}$,Fo,Sp,(Mo) |
| 4 | 43' | 675 | 2.0 | 330 | $Clin_{ss}$,$Di_{ss}$,Fo,Cc |
| | 411 | 890 | 2.0 | 214 | $Clin_{ss}$,$Di_{ss}$,Fo,?Sp |
| | 47 | 605 | 4.5 | 497 | $Clin_{ss}$,$Chl_{ss}$,Cc,? |
| | 300 | 900 | 5.0 | 22 | $Clin_{ss}$,$Di_{ss}$,Fo,?Sp |
| | 310 | 900 | 7.0 | 19 | $Clin_{ss}$,$Di_{ss}$,Fo,Sp |
| C | 169' | 800 | 2.0 | 268 | $Clin_{ss}$ |
| B | 168' | 800 | 2.0 | 268 | $Clin_{ss}$ |
| A | 167' | 800 | 2.0 | 268 | $Clin_{ss}$ |
| 5 | 44' | 675 | 2.0 | 330 | $Clin_{ss}$ |
| | 100' | 800 | 2.0 | 19 | $Clin_{ss}$ |
| | 390 | 865 | 2.0 | 240 | $Clin_{ss}$ |
| | 148 | 600 | 7.0 | 816 | $Clin_{ss}$ |
| D | 174' | 800 | 2.0 | 268 | $Clin_{ss}$ |
| | 379 | 975 | 5.0 | 23 | $Clin_{ss}$ |
| E | 339' | 865 | 2.0 | 121 | $Clin_{ss}$ |
| 6 | 446 | 600 | 2.0 | 1 | $Clin_{ss}$ |
| | 12 | 600 | 2.0 | 573 | $Clin_{ss}$ |
| | 45' | 675 | 2.0 | 330 | $Clin_{ss}$ |
| | 437 | 750 | 2.0 | 1/4 | $Clin_{ss}$ |
| | 445 | 750 | 2.0 | 128 | $Clin_{ss}$ |
| | 238 | 800 | 2.0 | 96 | $Clin_{ss}$ |
| | 149 | 600 | 7.0 | 816 | $Clin_{ss}$ |
| F | 324' | 850 | 2.0 | 122 | $Clin_{ss}$ |
| 7 | 440 | 750 | 2.0 | 4 | $Clin_{ss}$ |
| | 170' | 800 | 2.0 | 268 | $Clin_{ss}$ |
| | 371 | 750 | 7.0 | 332 | $Clin_{ss}$ |
| G | 341 | 875 | 2.0 | 121 | Sp,$Mel_{ss}$,An,Co |
| 8 | 588 | 690 | 2.0 | 1196 | $Clin_{ss}$,Co,Cc,?Sp |
| | 171 | 800 | 2.0 | 268 | $Clin_{ss}$,Sp,Co,? |
| | 342 | 875 | 2.0 | 121 | Sp,$Mel_{ss}$,Co,?$CA_6$ |
| 18 | 589 | 690 | 2.0 | 1196 | $Clin_{ss}$,Sp,Co,Cc |
| | 343 | 875 | 2.0 | 121 | Sp,$Mel_{ss}$,$CA_6$,$CA_2$ |

* cf. Table 1.

** Runs marked ' have been used to determine unit cell parameters of the clintonite mixed crystals.

*** All assemblages given coexist with a hydrous gas phase. Phases given in parentheses are considered to be metastable. Abbreviations used for synthesized phases: An, anorthite; $CA_2$, calciumdialuminate; $CA_6$, calciumhexaluminate; Cc, calcite; $Chl_{ss}$, chlorite solid solution; $Clin_{ss}$, clintonite solid solution; Co, corundum; $Di_{ss}$, diopside solid solution; Fo, forsterite; $Mel_{ss}$, melilite solid solution; Mo, monticellite; Sp, spinel.

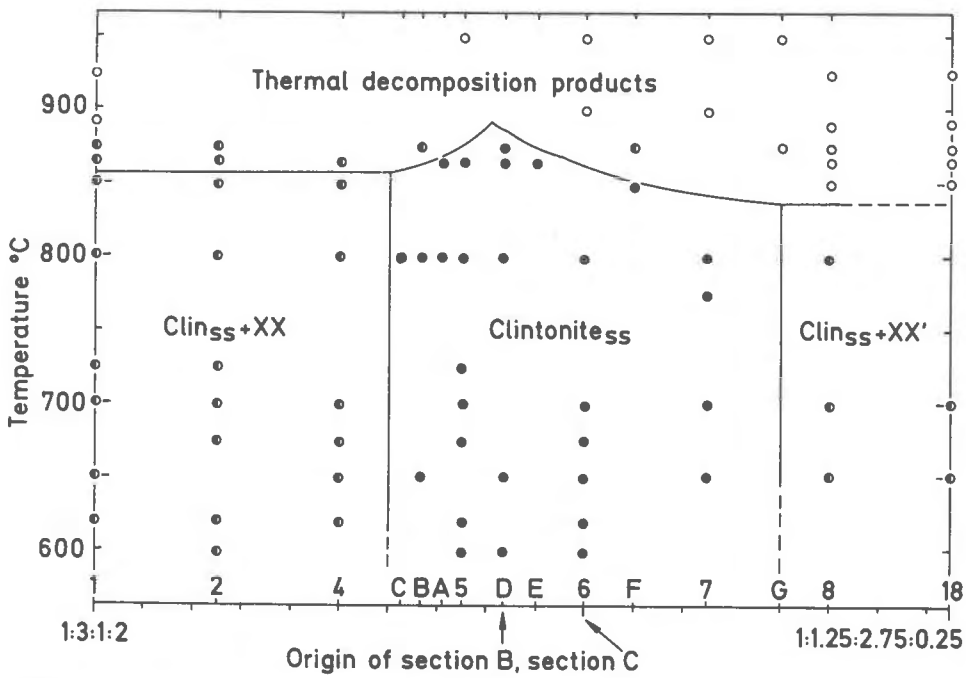


FIG. 3. *T-X* field of synthesis of clintonites on section A at $P_{H_2O}$ = 2 kbar. A hydrous gas phase is omnipresent. Dots: single-phase clintonite; half-filled circles: clintonite + other phases; open circles: clintonite-free assemblages. Numbers and letters just above the abscissa are the symbols of the starting materials (*cf* Table 1). Proportions given at the abscissa are the ratios CaO:MgO:$Al_2O_3$:SiO. **XX** and **XX'** stand for various phase assemblages that coexist with clintonite.

actual number of atoms are plotted against each other (Fig. 2).

On the basis of these results, the sections A, B, and C through the system CaO–MgO–$Al_2O_3$–$SiO_2$–$H_2O$ (*cf* Figs. 1, 2) have been chosen in order to delineate the field of solid solubility of trioctahedral (or nearly trioctahedral) calcium micas. The compositions investigated ranged as follows (dry oxide proportions given only):

A. CaO:3MgO:$Al_2O_3$:2$SiO_2$ – CaO:1.25MgO:2.75$Al_2O_3$:0.25$SiO_2$ (substitution $Mg^{VI}$ + $Si^{IV}$ = $Al^{VI}$ + $Al^{IV}$)

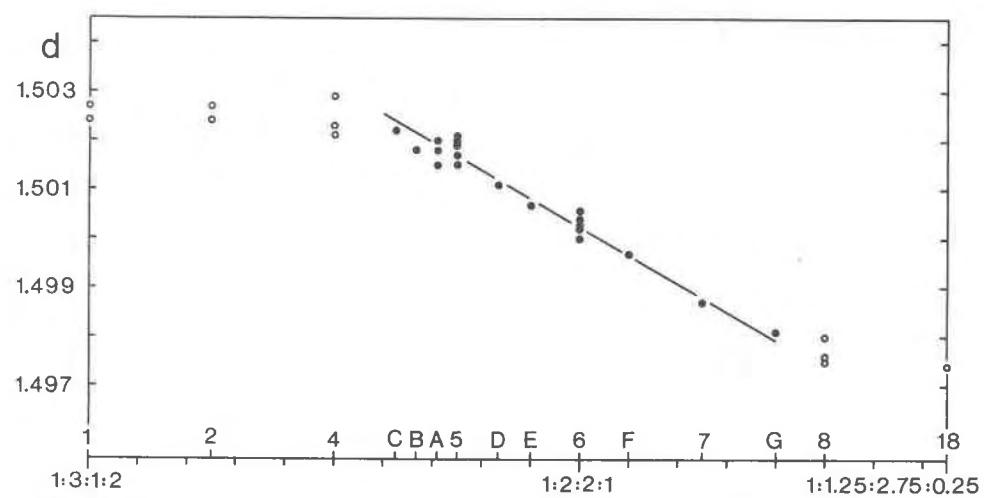


FIG. 4. Bulk composition on section A relative to *d* (in Å) for the *060,331* peak. The open circles indicate multiphase assemblages; filled circles indicate single-phase mixed crystals of clintonite coexisting with a hydrous gas phase. Numbers, letters, and portions at the abscissa as in Figure 3.

TABLE 3. Results of Critical Synthesis Runs on Sections B and C

| Composition* | Run No.** | T (°C) | $P_{H_2O}$ (Kbar) | Duration (Hours) | Condensed Phases Observed*** |
|---|---|---|---|---|---|
| Section B | | | | | |
| 34 | 592' | 650 | 2.0 | 714 | $Clin_{ss}$ |
| | 573' | 750 | 2.0 | 281 | $Clin_{ss}$ |
| 10 | 583' | 550 | 2.0 | 1295 | $Clin_{ss}$ |
| | 173 | 800 | 2.0 | 268 | $Clin_{ss}$ |
| | 545 | 990 | 5.0 | 69 | $Clin_{ss}$ |
| 35 | 574' | 750 | 2.0 | 281 | $Clin_{ss}$,An,?Co,?Sp |
| 9 | 582' | 550 | 2.0 | 1295 | $Clin_{ss}$,Co,? |
| | 172 | 800 | 2.0 | 268 | $Clin_{ss}$,Sp,? |
| | 546 | 990 | 5.0 | 69 | $Clin_{ss}$,An,Sp,? |
| Section C | | | | | |
| 33 | 591' | 650 | 2.0 | 714 | $Clin_{ss}$ |
| 31 | 569 | 550 | 2.0 | 2897 | $Clin_{ss}$ |
| | 552' | 650 | 2.0 | 807 | $Clin_{ss}$ |
| | 516 | 965 | 5.0 | 66 | $Clin_{ss}$,An,Co,?Sp |
| 32 | 590' | 650 | 2.0 | 714 | $Clin_{ss}$ |
| | 576' | 750 | 2.0 | 281 | $Clin_{ss}$ |
| 30 | 553' | 650 | 2.0 | 807 | $Clin_{ss}$,An,Co |
| | 524 | 700 | 2.0 | 695 | $Clin_{ss}$,?An,?Co |
| | 548' | 740 | 2.0 | 77 | $Clin_{ss}$ |
| | 515 | 965 | 5.0 | 66 | $Clin_{ss}$,An,Sp,? |
| 29 | 567 | 550 | 2.0 | 2897 | $Clin_{ss}$,An,Co |
| | 549' | 740 | 2.0 | 77 | $Clin_{ss}$,An,Co |
| 28 | 483 | 480 | 2.0 | 1343 | $Clin_{ss}$,$Marg_{ss}$ |
| | 566 | 550 | 2.0 | 2897 | $Clin_{ss}$,An,Co |
| | 523 | 700 | 2.0 | 695 | $Clin_{ss}$,An,Co |
| 27 | 482 | 480 | 2.0 | 1343 | $Clin_{ss}$,$Marg_{ss}$ |
| | 564 | 550 | 2.0 | 2683 | $Clin_{ss}$,An,Co |

* cf. Table 1.

** Runs marked ' have been used to determine unit cell parameters of the clintonite mixed crystals.

*** All assemblages given coexist with a hydrous gas phase. Abbreviations used see Table 2, in addition: $Marg_{ss}$, margarite solid solution.

B. $CaO:2.17MgO:1.83Al_2O_3:1.17SiO_2$ – $CaO:1.83MgO:1.83Al_2O_3:1.33SiO_2$ (substitution $2\,Mg^{VI} + Al^{IV} = Al^{VI} + Si^{IV}$)

C. $CaO:2MgO:2Al_2O_3:SiO_2$ – $CaO:MgO:2Al_2O_3:1.5\,SiO_2$ (substitution $2\,Mg^{VI} + Al^{IV} = Al^{VI} + Si^{IV}$)

## Experimental Results

Synthesis experiments on the three joins listed above were performed at water pressures of 1 to 7 kbar and temperatures between 300 and 1200°C. The bulk of the data was obtained in isobaric *T-X* sections at 2 kbar, with run durations up to 2897 hours. This pressure has been selected since, for most natural clintonite occurrences, pressures of this order of magnitude are to be assumed (Forman, Kodama, and Abbey, 1967a). The calculated composition of the starting materials (water- and $CO_2$-free) and the equivalent structural formulae of hypothetical micas are listed in Table 1.

### *Section A: Trioctahedral Ca-micas, Substitution MgSi → 2Al*

Starting from the Ca analog of phlogopite ($CaO:3MgO:Al_2O_3:2SiO_2:H_2O$), this substitution forms less-siliceous micas with fully trioctahedral occupancy. The general formula of calcium micas in the system investigated is $Ca(Mg_xAl_y)(Al_{4-z}Si_zO_{10})(OH)_2$. For micas on section A, $x = 1 + z$ and $y = 2 - z$. Runs critical for the present investigation of solid solubility are listed in Table 2. Results of 2 kbar runs are shown graphically in the *T-X* section of Figure 3. The high-temperature breakdown products of clintonite as well as the coexisting phases at lower temperatures will be treated in a subsequent paper on stability relations.

Despite runs of up to 115 days duration, disequilibrium assemblages have been obtained below 600°C. At higher temperatures, however, the results are considered to represent equilibrium phase relations, since phase assemblages and amounts of phases were found to be independent of run duration and because the upper stability limit of the clintonites could be reversed (Olesch, 1972).

### *T-X Region of Homogeneous Clintonite Solid Solutions*

In the central part of the *T-X* diagram (Fig. 3), clintonite forms the only solid phase at temperatures up to 870°C. Thus, the chemical composition of these micas corresponds to the bulk composition of the charge (Table 1). The presence of the required 2(OH) per formula unit was checked by thermal gravimetric analysis; a single-phase product obtained from composition 6 (Table 1) yielded 4.1 wt percent water (theoretical value 4.3 wt percent). As can be seen from Table 2 and Figure 3, single-phase micas of the general composition $Ca(Mg_{1+z}Al_{2-z})(Al_{4-z}Si_zO_{10})(OH)_2$ could only be grown in the range $1.4 > z > 0.6$. The Ca analog of phlogopite ($z = 2$) could not be prepared.

As an additional criterion for the limits of solid solubility on this join, the X-ray properties of the clintonites have been used. Although multiply in-

dexed, the reflection $\bar{3}14, 060, \bar{3}31$ well suits this purpose, since it shifts strongly with $z$, and does not interfere with reflections of other phases present. In addition, the contributions of *060* and $\bar{3}31$ to this peak are independent of stacking disorder, since $k = 3n$ (Takeuchi, 1965; Takeuchi and Sadanaga, 1966). The contribution of $\bar{3}14$ to this peak is very small (Borg and Smith, 1969) and the difference in $d$ between *060* and $\bar{3}31$ calculated from the lattice constants given below is, on the average, only 0.0003 Å and, within limits of error, not systematically related to composition. Therefore, the position of the composite peak can be used with confidence. Its $d$ values, plotted in Figure 4 as a function of bulk composition, decrease with decreasing Si content in the homogeneous samples but are, within the limits of error, constant in the adjoining multiphase regions of the *T-X* section. The limits of solid solubility derived above from phase analysis are thus reconfirmed. They are only in fair agreement with those reported by Velde (1973) for the same join. The reasons for the discrepancies cannot be discussed at the moment, because Velde (1973) does not give the actual data points.

At least at temperatures above 600°C, the limits of solid solubility have not been found to be a function of temperature until the upper thermal stability limit at some 870°C is attained. Similarly it could be shown that, on the MgSi-rich side of the join, pressures up to 7 kbar do not shift the limit of solid solubility significantly (*cf* Table 2). Pressure dependence of solid solubility on the Al-rich side has not been checked systematically.

### *Solid Solubility below 600°C*

At relatively low temperatures, the synthesis field of single-phase clintonites shrinks, mainly on the Al-rich side of the section A. For instance, at 530°C, 2 kbar, the only single-phase products encountered on this join are poorly crystalline or disordered clintonites (see below) of composition $z = 1.2$ to $z = 1.15$. It is at present not clear whether this asymmetric diminution of the synthesis field of clintonite solid solution reflects metastability or instability of the limiting compositions $z = 0.6$ and 1.4 at higher temperatures.

### *Sections B and C: Solid Solubility towards Dioctahedral Micas*

As discussed above, natural trioctahedral calcium micas can exhibit limited solid solubility towards dioctahedral calcium micas. Sections B and C served for studying these relationships, using the substitution $2Mg^{VI} + Al^{IV} = Si^{IV} + Al^{VI}$. In the general formula cited earlier, $x = 4.5 - 2z$ and $y = z - 0.33$ for section B but $x = 4 - 2z$ and $y = z$ for section C. Section B starts from section A at $z = 1.17$, whereas C starts at $z = 1.0$. It should be pointed out, that only join C leads directly towards margarite, whereas B is terminated at a hypothetical dioctahedral end member $Ca(Mg_{0.17}Al_{1.83})(Al_{1.83}Si_{2.17}O_{10})(OH)_2$. Critical runs for both joins are listed in Table 3.

Single-phase clintonites on join B could only be synthesized up to $z = 1.27$. Variation with composition of $d$ for $060, \bar{3}31$ is too small on this section to be used as a criterion for the limit of solid solubility. It varies only 1.4981 Å at $z = 1.17$ to 1.4988 at $z = 1.27$. Therefore, the dependence of lattice constants on composition along this section was established first from the homogeneous phases (see below). The limit of solid solubility was derived from the lattice constants $b$ and $V$ of clintonites in polyphase assemblages obtained on more siliceous bulk compositions of the section (Fig. 5, left). The effect of temperature on the solid solubility, if any, is slight, the most siliceous mica ($z = 1.27$) having an octahedral cation deficiency of about 3 percent.

Section C exhibits markedly higher and distinctly temperature-dependent solid solubility of the clintonite phase (Table 3; Fig. 5, right). The limits of solid solubility were, again, derived from the lattice constants. At 550°C and 2 kbar, the field of clintonite solid solutions extends from $z = 1.0$ to $z = 1.17$; at 800°C it extends up to $z = 1.24$, corresponding to an increase of the margarite component with temperature from 17 to 24 mole percent.

## Solid Solubility and Properties of Synthetic Clintonites as Compared with the Natural Mineral Phases

### *Solid Solubility*

These experiments and X-ray data show that the field of homogeneous clintonite mixed crystals can, at suitable *P-T-X* conditions, extend to the following limiting compositions: $Ca(Mg_{2.4}Al_{0.6})(Al_{2.6}Si_{1.4}O_{10})(OH)_2$ to $Ca(Mg_{1.6}Al_{1.4})(Al_{3.4}Si_{0.6}O_{10})(OH)_2$ along section A; $Ca(Mg_{2.17}Al_{0.83})(Al_{2.83}Si_{1.17}O_{10})(OH)_2$ to $Ca(Mg_{1.97}Al_{0.93})(Al_{2.73}Si_{1.27}O_{10}(OH)_2$ along section B; $Ca(Mg_2Al)(Al_3SiO_{10})(OH)_2$ to $Ca(Mg_{1.53}Al_{1.24})(Al_{2.76}Si_{1.24}O_{10})(OH)_2$ along section C. Temperature affects only the solid solubility towards dioctahedral micas (sections B and C). The estimated extension of the field of synthetic clintonites is shown (Fig. 6) in terms of number of silicon atoms and octahedral occupancy, and compared to the natural phases. The

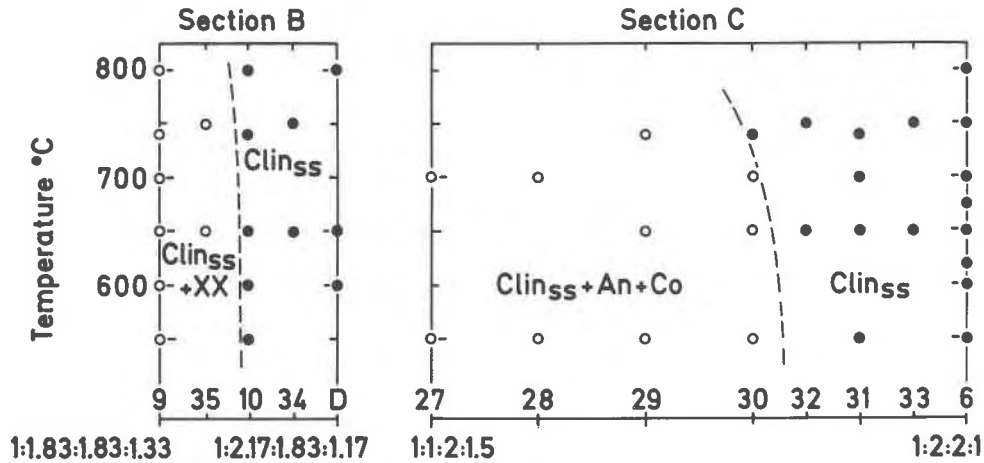


FIG. 5. *T-X* diagrams for section B (left), and section C (right) at $P_{H_2O}$ = 2 kbar. A hydrous gas phase is omnipresent. Dots: single-phase clintonite; open circles: clintonite + other phases. For abbreviations see Table 2; **XX** stands for various phase assemblages that coexist with clintonite. Numbers and letters just above the abscissae are the symbols of the starting materials (*cf* Table 1). Proportions given at the abscissae are the ratios $CaO:MgO:Al_2O_3:SiO_2$.

solid solubility encountered in the synthetic system encompasses and, on the Al-rich side, considerably exceeds the variation encountered in natural clintonites.

*Physical Properties*

The synthetic clintonites form a felt of interlocked platy crystals of very small grain size (at most 3 $\mu$m diameter). The scanning electron microscope showed the subhexagonal shape of these plates. No twinning has been observed. Only a mean refractive index $(\beta + \gamma)/2$ of 1.658 ± 0.002 (composition $z$ = 1.0, section A) could be determined, which agrees with the data reported for natural clintonites. Its variation with chemical composition is only slight.

As expected, the synthetic micas are colorless. Natural clintonites, on the other hand, show colors from dark green to colorless or to brown, due to $Fe^{2+}$–$Fe^{3+}$ and $Ti^{3+}$–$Ti^{4+}$ charge transfer bands, respectively, according to Manning (1969).

The X-ray powder patterns could be indexed on the basis of a 1*M* cell (Takeuchi, 1965; Takeuchi and Sadanaga, 1966). No indications of a $2M_1$ polytype (Machatschki and Mussgnug, 1942) were encountered. The powder data obtained agree closely with those calculated by Borg and Smith (1969) for natural material. There is also general agreement of the calculated and observed intensities of the peaks (Table 4).

On the other hand, the intensity of *hkl* reflections depends on bulk composition as well as on physical conditions of synthesis. Keeping pressure, temperature, and run duration constant, *hkl* peaks are much stronger in the Al-rich than in the Al-poor members of the solid solution series, whereas relative intensities of *h00, 0k0, 00l,* and *20l* reflections are not affected significantly. This indicates increasing stacking disorder with decrease in both tetrahedral and octahedral aluminum (Smith and Yoder, 1956). As to be expected from results of Yoder and Eugster (1955) on synthetic muscovites, stacking disorder in the synthetic micas of the present study should depend strongly on duration and temperature of the runs. Figure 7 shows the increase with time of the relative intensity of the $\bar{1}13$ reflection of a clintonite

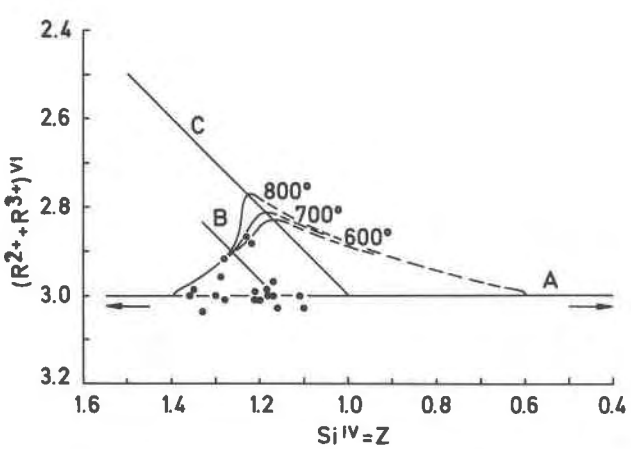


FIG. 6. Limit of clintonite solid solubility as a function of temperature at 2 kbar (solid and dashed curves) in the plot $(R^{2+} + R^{3+})^{VI}$ *vs* $Si^{IV}$. The black dots represent compositions of natural clintonites (*cf* Fig. 2).

$Ca(Mg_2Al)(Al_3SiO_{10})(OH)_2$ at two different temperatures. Whereas at 750°C an equilibrium value is obviously attained after some 100 hours, the intensity of this reflection and thus also the degree of stacking order is generally lower and increases even after some 600 hours at 600°C.

A selection of lattice constants of synthetic clintonites is compiled in Table 5. Taking into account all determinations made on single-phase clintonites, the following regression equations have been obtained for the three sections.[1]

Section A (11 data points on 9 different compositions):

$$a = 0.020(4)z + 5.171(5)\ \text{Å}$$
$$b = 0.034(4)z + 8.960(5)\ \text{Å}$$
$$c = 0.028(6)z + 9.770(7)\ \text{Å}$$
$$V = 4.75(53)z + 445.51(60)\ \text{Å}^3$$
$$\beta = 100.16(2)°$$

Section B (6 data points on 3 different compositions):

$$a = -0.044(5)z + 5.247(6)\ \text{Å}$$
$$b = -0.031(16)z + 9.032(19)\ \text{Å}$$
$$c = -0.128(26)z + 9.955(32)\ \text{Å}$$
$$V = -8.27(88)z + 460.54(1.04)\ \text{Å}^3$$
$$\beta = 100.17(2)°$$

Section C (9 data points on 5 different compositions):

$$a = -0.038(6)z + 5.229(6)\ \text{Å}$$
$$b = -0.074(13)z + 9.068(14)\ \text{Å}$$
$$c = -0.060(10)z + 9.857(11)\ \text{Å}$$
$$V = -9.82(75)z + 460.05(82)\ \text{Å}^3$$
$$\beta = 100.16(2)°$$

The monoclinic angle $\beta$ does not vary systematically with composition. The other lattice constants decrease linearly with increasing Al content (section A) and admixture of a dioctahedral component (sections B and C). Inclusion of a quadratic $z$ term did not improve the fit significantly. In general the lattice constants obtained agree fairly well with those

TABLE 4. X-Ray Powder Data of Synthetic Clintonite $Ca(Mg_{2.1}Al_{0.9})(Al_{2.9}Si_{1.1}O_{10})(OH)_2$

| h | k | l | $d_{obs}$ | $d_{calc}$ | $(Q_{obs}-Q_{calc})\times10^5$ | $I/I_o$ | $I_{calc}$** |
|---|---|---|---|---|---|---|---|
| 0 | 0 | 1 | 9.644 | 9.645 | 0 | 21 | 22 |
| 0 | 2 | 0 | 4.493 | 4.498 | 12 | 5 | 4 |
| 0 | 2 | 1 | 4.079 | 4.077 | -6 | 2 | 2 |
| 1 | 1 | 1 | 3.821 | 3.820 | -4 | 6 | 15 |
| -1 | 1 | 2 | 3.556 | 3.550 | -26 | 11 | 32 |
| 0 | 2 | 2 | 3.289 | 3.289 | 2 | 14 | 39 |
| 0 | 0 | 3 | 3.215 | 3.215 | 2 | 78 | 48 |
| 1 | 1 | 2 | 3.042 | 3.044 | 13 | 13 | 40 |
| -1 | 1 | 3 | 2.820 | 2.818 | -18 | 10 | 26 |
| 0 | 2 | 3 | 2.615 | 2.616 | 6 | 6 | 16 |
| 1 | 3 | 0 | 2.586 | 2.586 | 8 | 13 | 12 |
| -2 | 0 | 1 | | 2.586 | -1 | | |
| -1 | 3 | 1 | 2.556 | 2.556 | 1 | 100 | 100 |
| 2 | 0 | 0 | | 2.556 | -3 | | |
| 1 | 3 | 1 | 2.442 | 2.444 | 28 | 22 | 18 |
| -2 | 0 | 2 | | 2.443 | 14 | | |
| 2 | 0 | 1 | 2.369 | 2.369 | 1 | 14 | 12 |
| -1 | 3 | 2 | | 2.369 | 0 | | |
| 1 | 3 | 2 | 2.199 | 2.199 | 8 | 15 | 17 |
| -2 | 0 | 3 | | 2.198 | -10 | | |
| 2 | 0 | 2 | 2.109 | 2.110 | 11 | 50 | 46 |
| -1 | 3 | 3 | | 2.109 | 5 | | |
| 0 | 4 | 2 | 2.038 | 2.038 | 6 | 2 | 6 |
| 1 | 3 | 3 | 1.9290 | 1.9328 | 107 | 18 | 12 |
| -2 | 0 | 4 | | 1.9320 | 83 | | |
| 0 | 0 | 5 | | 1.9290 | 0 | | |
| 2* | 0 | 3 | 1.8475 | 1.8481 | 20 | 8 | 5 |
| -1 | 3 | 4 | | 1.8478 | 9 | | |
| 1 | 3 | 4 | 1.6900 | 1.6901 | 5 | 7 | 4 |
| -2 | 0 | 5 | | 1.6894 | -23 | | |
| 2 | 0 | 4 | 1.6176 | 1.6173 | -17 | 19 | 20 |
| -1 | 3 | 5 | | 1.6170 | -33 | | |
| 0 | 0 | 6 | 1.6078 | 1.6075 | -16 | 4 | 5 |
| 3 | 1 | 1 | 1.6042 | 1.6032 | -49 | 3 | 7 |
| -3 | 1 | 3 | | 1.6028 | -69 | | |
| 1 | 5 | 2 | 1.5725 | 1.5724 | -4 | 2 | 6 |
| -2 | 4 | 3 | | 1.5720 | -23 | | |
| 2 | 4 | 2 | 1.5391 | 1.5386 | -27 | 1 | 4 |
| -1 | 5 | 3 | | 1.5385 | -33 | | |
| -3 | 1 | 4 | 1.4995 | 1.5023 | 170 | 41 | 40 |
| 0 | 6 | 0 | | 1.4994 | -3 | | |
| -3 | 3 | 1 | | 1.4990 | 24 | | |
| 1 | 3 | 5 | 1.4843 | 1.4842 | -11 | 28 | 26 |
| -2 | 0 | 6 | | 1.4836 | -44 | | |
| 0 | 6 | 3 | 1.3589 | 1.3589 | 1 | 8 | 6 |
| 3 | 3 | 2 | | 1.3588 | -6 | | |
| -3 | 3 | 4 | | 1.3584 | -35 | | |

* Conditions of synthesis: 865° C, 2 Kbar, 121 hours.
X-ray diffractogram with internal Si standard.

** I(PK) Borg and Smith (1969, p. 613)

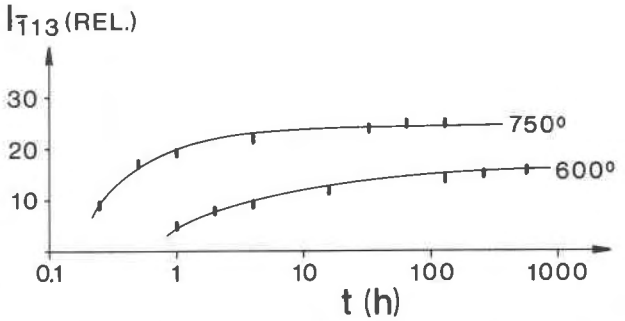


FIG. 7. Relationship between the relative intensity of the $\bar{1}13$ peak and run duration at 2 kbar, 600°C and 750°C, respectively; composition $Ca(Mg_2Al)(Al_3SiO_{10})(OH)_2$. Low relative intensities of the $\bar{1}13$ peak indicate stacking disorder.

[1] The parenthesized figures represent the estimated standard deviation (esd) in terms of least units cited for the value to their immediate left; thus, 5.171(5) indicates an esd of 0.005. The number of silicons per formula unit is represented by $z$.

TABLE 5. Selection of Unit Cell Parameters of Single Phase, Mixed Crystals of Clintonite from Sections A, B, and C

| Composition* | Run No.** | a (Å) | b (Å) | c (Å) | β (°) | V (Å$^3$) |
|---|---|---|---|---|---|---|
| Section A | | | | | | |
| C | 169 | 5.2002(9)*** | 9.0075(16) | 9.8061(23) | 100.18(2) | 452.084(133) |
| B | 168 | 5.1956(18) | 9.0045(32) | 9.8010(33) | 100.15(2) | 451.356(237) |
| A | 389 | 5.1942(15) | 9.0044(23) | 9.8077(29) | 100.13(2) | 451.560(196) |
| 5 | 100 | 5.1984(13) | 9.0027(21) | 9.8101(28) | 100.18(2) | 451.888(167) |
| E | 339 | 5.1924(13) | 8.9964(21) | 9.7982(27) | 100.15(2) | 450.538(171) |
| 6 | 45 | 5.1908(19) | 8.9970(32) | 9.7956(41) | 100.13(3) | 450.332(270) |
| F | 324 | 5.1884(13) | 8.9924(22) | 9.7906(22) | 100.18(2) | 449.768(161) |
| 7 | 170 | 5.1878(9) | 8.9852(15) | 9.7936(27) | 100.18(1) | 449.191(130) |
| Section B | | | | | | |
| 34 | 573 | 5.1935(9) | 8.9959(14) | 9.8005(17) | 100.17(1) | 450.684(103) |
| 10 | 555 | 5.1920(14) | 8.9921(23) | 9.7982(32) | 100.18(2) | 450.251(187) |
| Section C | | | | | | |
| 33 | 575 | 5.1894(9) | 8.9879(15) | 9.7957(19) | 100.16(1) | 449.721(113) |
| 31 | 547 | 5.1890(8) | 8.9857(16) | 9.7901(19) | 100.18(1) | 449.297(122) |
| 32 | 590 | 5.1845(11) | 8.9833(16) | 9.7879(22) | 100.17(2) | 448.692(138) |
| 30 | 548 | 5.1843(10) | 8.9768(19) | 9.7818(22) | 100.17(2) | 448.084(145) |

* see Table 1.

** see Table 2 and Table 3.

*** Parenthesized figures represent the estimated standard deviation (esd) in terms of least units cited for the value to their immediate left, thus 5.2002(9) indicates an esd of 0.0009.

reported for natural clintonites (Table 6), the latter being, however, slightly, but systematically, higher:

| | natural clintonites | synthetic clintonites |
|---|---|---|
| *a* | 5.19 – 5.25 Å | 5.18 – 5.20 Å |
| *b* | 9.00 – 9.03 Å | 8.97 – 9.01 Å |
| *c* | 9.80 – 9.97 Å | 9.78 – 9.81 Å |

Probably this difference stems from the presence of additional large cations ($Fe^{2+}$, $Fe^{3+}$, Na, Ba) in the natural phases. The systematically higher densities of natural clintonites, ranging from 3.035 (Kokscharow, 1875) to 3.081 g cm$^{-3}$ (Eakle, 1916), as compared to densities calculated from unit cell data for the synthetic micas—2.936 to 2.969 g cm$^{-3}$—may be similarly explained.

TABLE 6. Unit Cell Parameters of Natural 1*M* Clintonites, Taken from the Literature

| a (Å) | b (Å) | c (Å) | β (°) | Authors; locations |
|---|---|---|---|---|
| 5.204 | 9.026 | 9.812 | 100.33 | Forman et al (1967a); Shishimskaja Gora, Slatoust |
| 5.216 | 9.012 | 9.854 | 100.08 | ibid.; Nikolaje Maximilianowsk, Achmatowsk, Ural |
| 5.25 | 9.00 | 9.81 | 100.17 | Forman*(1951); ibid. |
| 5.215 | 9.013 | 9.853 | 100.07 | ibid.; Crestmore, Calif. |
| 5.21 | 9.02 | 9.97 | 100.05 | Sanero (1940); Lago della Vacca, Adamello, Alps |
| 5.19 | 9.00 | 9.80 | 100.13 | Stevenson and Beck (1965); Tobacco Root Mountains, Mont. |
| 5.194 | 9.003 | 9.802 | 100.10 | Takeuchi (1965); Chichibu Mine, Japan |

* Values given by Forman (1951) in KX units have been recalculated into Å units.

### *Crystal Chemical Properties*

The most interesting crystal chemical features of both synthetic and natural clintonites are (1) complete or nearly complete occupancy of the interlayer position by Ca; (2) rather limited solid solubility towards dioctahedral micas; and (3) a ratio of $Si/Al^{IV}$ of less than one.

The small Ca cation in the interlayer causes a distinct contraction of the mica structure in the *c* direction, compared to the alkali micas (Hazen and Wones, 1972), as well as a diminution of the *b* dimension (Radoslovich, 1962). Natural clintonites exhibit an octahedral occupancy between 3.04 and 2.87, which is a slightly smaller variation than encountered in the synthetic system (3.0 – 2.76). Ordering among octahedral Mg,Al and (possibly) vacancies in the clintonites is not very well understood at present. In most micas the smaller trivalent cations are concentrated in the two topologically equivalent octahedral sites, the divalent cation preferring the third, structurally distinct site (Veitch and Radoslovich, 1963). These relationships are, according to Takeuchi (1965) and Takeuchi and Sadanaga (1966), just reversed in the trioctahedral calcium micas. This might explain the rather limited solid solubility towards dioctahedral micas.

The trioctahedral calcium micas show extremely

TABLE 7. Calculated Tetrahedral Layer Rotation $\alpha$ in the End Members of the Sections Investigated

| Section | $Al^{IV}$ (±.05) | $d_t$(Å)* (±.002) | b(Å)** (±.002) | ∝(calc) according to Radoslovich and Norrish (1962) (±0.2°) | ∝(calc) according to Hazen and Wones (1972) (±0.4°) |
|---|---|---|---|---|---|
| A | 2.6 | 1.718 | 9.008 | 22.1 | 22.0 |
| | 3.4 | 1.748 | 8.981 | 25.1 | 24.7 |
| B | 2.83 | 1.726 | 8.996 | 22.9 | 22.8 |
| | 2.73 | 1.723 | 8.993 | 22.7 | 22.7 |
| C | 3.0 | 1.732 | 8.994 | 23.6 | 23.4 |
| | 2.76 | 1.724 | 8.977 | 23.0 | 22.7 |

* The average tetrahedral bond length $d_t$ has been obtained by linear interpolation of the data by Smith and Bailey (1963) given for layer silicates.

** b of clintonites synthesized in the present study has been taken from the regression equations (cf. text).

low $Si/Al^{IV}$ ratios, from 1.4:2.6 down to 0.6:3.4. The large amount of Al distributed randomly over the tetrahedral sites (Takeuchi and Sadanaga, 1966; Farmer and Velde, 1973) increases the size of the tetrahedra compared to other, more siliceous, layer lattice silicates. To account for the different unit size of octahedral and tetrahedral layers, the tetrahedra have to rotate around their trigonal axis, which is perpendicular to (001). The angle of this rotation can be calculated either from the relation $\alpha$ = arc cos $(b_{obs}/(9.051 + 0.254\ X)$ where $X$ = number of Al atoms per 4 tetrahedral sites (Radoslovich and Norrish, 1962), or from $\alpha$ = arc cos $(b_{obs}/4 \cdot \sqrt{2} \cdot d_t)$ where $d_t$ = average tetrahedral bond length (Hazen and Wones, 1972). Such calculations for $\alpha$ (Table 7) agree with the value reported by Takeuchi (1965) for clintonite (23°). They show that $\alpha$ increases with a decrease of the $Si/Al^{IV}$ ratio. These rotations are the largest calculated so far for layer lattice silicates. On the other hand $\alpha$ decreases on introduction of a dioctahedral component into the mica structure, approaching the value for margarite (21°; Takeuchi, 1965).

The presence of 65 to 85 percent Al on the tetrahedral sites necessitates the existence of an unusually large number of tetrahedral Al-O-Al bonds, which is at variance with Loewensteins' statement (1954) that such bonds are energetically unfavorable and should not occur. Similar violations of Loewensteins' rule have recently been reported by Moore (1969), Gebert (1972), and Lin and Burley (1973).

## Acknowledgments

The present paper forms part of a general study of trioctahedral calcium micas performed at Kiel University and accepted as a thesis by Ruhr-University Bochum. I thank F. Seifert for helpful discussions during the course of the study. Provision of laboratory facilities at Mineralogisches Institut, Kiel University, by the late F. Karl and at the Institut für Mineralogie, Ruhr-University Bochum, by W. Schreyer are gratefully acknowledged. The paper has had the benefit of review by P. K. Hörmann, Kiel; K. Langer, Bochum; and F. Seifert, Kiel.

## References

AKHUNDOV, Y. A., K. S. MAMEDOV, AND N. V. BELOV (1961) Crystal structure of brandisite. *Dokl. Akad. Nauk. SSSR,* **137,** 167–170 (in Russian).

BIANCHI, A., AND O. HIEKE (1946) La xantofillite dell'Adamello meridionale. *Period. Mineral.* **15,** 87–146.

BORG, J. Y., AND D. K. SMITH (1969) Calculated X-ray powder patterns for silicate minerals. *Geol. Soc. Am. Mem.* **122,** 896 p.

BURNHAM, C. W. (1962) Lattice constant refinement. *Carnegie Inst. Wash. Year Book,* **61,** 132–135.

CHRISTOPHE-MICHEL-LÉVY, M. (1964) Synthèses hydrothermales dans le système gehlénite–akermanite, $Ca_2Al_2SiO_7$–$Ca_2MgSi_2O_7$ en milieu carbonaté. *Bull. Soc. franc. Minéral. Cristallogr.* **87,** 28–30.

CLARKE, F. W., AND E. A. SCHNEIDER (1892) Experiments upon the constitution of certain micas and chlorites. *Am. J. Sci.* **143,** 378–386.

CROWLEY, M. S., AND R. ROY (1964) Crystalline solubility in the muscovite and phlogopite groups. *Am. Mineral.* **49,** 348–362.

DOELTER, C. (1917) *Handbuch der Mineralchemie.* Bd. II, 2. Abteilung, Verl. Th. Steinkopff, Dresden und Leipzig. 1144 pp.

EAKLE, A. S. (1916) Xanthophyllite in crystalline limestone. *J. Wash. Acad. Sci.* **6,** 332-335.

FARMER, V. C., AND B. VELDE (1973) Effects of structural order and disorder on the infrared spectra of brittle micas. *Mineral. Mag.* **39,** 282–288.

FORMAN, S. A. (1951) Xanthophyllite. *Am. Mineral.* **36,** 450-457.

———, H. KODAMA, AND S. ABBEY (1967a) A re-examination of xanthophyllite (clintonite) from the type locality. *Can. Mineral.* **9,** 25–30.

———, ———, AND J. A. MAXWELL (1967b) The trioctahedral brittle micas. *Am. Mineral.* **52,** 1122–1128.

FRENCH, B. M., AND H. P. EUGSTER (1965) Experimental control of oxygen fugacities by graphite-gas equilibriums. *Geophys. Res.* **70,** 1529–1539.

GEBERT, W. (1972) Die Kristallstruktur von $Ba_{13}Al_{22}Si_{10}O_{66}$. *Z. Kristallogr.* **35,** 437–452.

HAMILTON, D. L., AND C. M. B. HENDERSON (1968) The preparation of silicate compositions by a gelling method. *Mineral. Mag.* **36,** 832–838.

HARADA, K., H. KODAMA, AND T. SUDO (1965) New mineralogical data for xanthophyllite from Japan. *Can. Mineral.* **8,** 255–262.

HAZEN, R. M., AND D. R. WONES (1972) The effect of cation substitution on the physical properties of trioctahedral micas. *Am. Mineral.* **57,** 103–129.

HINTZE, C. (1897) *Handbuch der Mineralogie.* Bd. 2, *Silikate und Titanate.* Verl. von Veit, Leipzig. 1841 p.

HUEBNER, J. S. (1971) Buffering techniques for hydrostatic systems at elevated pressures. In, J. C. Ulmer, Ed., *Research Techniques for High Pressure and High Temperatures,* Springer Verlag, New York.

ITO, J., AND J. E. AREM (1970) Idocrase; synthesis, phase relations and crystal chemistry. *Am. Mineral.* **55,** 880–912.

KOCH, G. (1935) Chemische und physikalisch-optische Zusammenhänge innerhalb der Sprödglimmergruppe. *Chemie der Erde,* **9,** 453–463.

KOKSCHAROW, N. (1875) Materialien zur Mineralogie Russlands. Zweiter Anhang zum Xanthophyllit. *Waluewit.* Vol. VII, 346–374, St. Petersburg.

LAITAKARI, A. (1921) Über die Petrographie und Mineralogie der Kalksteinlagerstätten von Parainen (Pargas). *Bull. Comm. Geol. Finlande,* **54,** 113 pp.

LIN, S. B., AND B. J. BURLEY (1973) The crystal structure of meionite. *Acta Crystallogr.* **B29,** 2024–2026.

LOEWENSTEIN, W. (1954) The distribution of aluminum in the tetrahedra of silicates and aluminates. *Am. Mineral.* **39,** 92–96.

LUTH, W. C., AND O. F. TUTTLE (1963) Externally heated cold-seal pressure vessels for use to 10,000 bars and 750°C. *Am. Mineral.* **48,** 1401–1403.

MACHATSCHKI, F., AND F. MUSSGNUG (1942) Über die Kristallstruktur des Chloritoids. *Naturwissenschaften,* **30,** 106.

MANNING, P. G. (1969) On the origin of colour and pleochroism of astrophyllite and brown clintonite. *Can. Mineral.* **9,** 663–677.

MOORE, P. B. (1969) The crystal structure of sapphirine. *Am. Mineral.* **54,** 31–49.

NIKOLAJEW, P. D. (1883) Chemische Zusammensetzung des Walujewits (abstr.). *Z. Kristallogr.* **7,** 634–635.

——— (1884) Zusammensetzung des Xanthophyllits (abstr.). *Z. Kristallogr.* **9,** 579–580.

OLESCH, M. (1972) Synthese und obere Stabilität von trioktaedrischen Calciumglimmern (Clintonit, Xanthophyllit) (abstr.). *Fortschr. Mineral.* **50,** Beiheft 1, 75–77.

——— (1973) *Synthese und Stabilität trioktaedrischer Calciumglimmer (Clintonit, Xanthophyllit, Brandisit).* Thesis, Ruhr-Universität Bochum.

PETERS, T. (1970) A simple device to avoid orientation effects in x-ray. *Norelco Rep.* **17,** 23–24.

RADOSLOVICH, E. W. (1962) The cell dimensions and symmetry of layer-lattice silicates. II. Regression relations. *Am. Mineral.* **47,** 617–636.

———, AND K. NORRISH (1962) The cell dimensions and symmetry of layer-lattice silicates. I. Some structural considerations. *Am. Mineral.* **47,** 599–616.

ROY, R., AND O. F. TUTTLE (1961) Investigations under hydrothermal conditions. In, L. H. Ahrens, K. Rankama, and S. K. Runcorn, Eds., *Physics and Chemistry of the Earth,* Vol. 1. Pergamon Press, Oxford. p. 138–180.

SANERO, E. (1940) La struttura della xantofillite. *Period. Mineral.* **11,** 53–77.

SEIFERT, F. (1970) *Das petrogenetische $P_{H_2O}$-T-Netz des Systems $MgO$–$Al_2O_3$–$SiO_2$–$H_2O$ im Druck-Temperatur-Bereich 0-7 Kb, 400–1250°C.* Habilitationsschrift, Ruhr-Universität Bochum, 154 pp.

SMITH, J. V., AND S. W. BAILEY (1963) Second review of Al–O and Si–O tetrahedral distances. *Acta Crystallogr.* **16,** 801–811.

———, AND H. S. YODER, JR. (1956) Experimental and theoretical studies of the mica polymorphs. *Mineral. Mag.* **31,** 209–235.

STEVENS, R. E. (1947) A system for calculating analyses of micas and related minerals to end members. *U.S. Geol. Surv. Bull.* **950,** 101–119.

STEVENSON, R. G., AND C. W. BECK (1965) Xanthophyllite from the Tobacco Root Mountains, Montana. *Am. Mineral.* **50,** 292–293.

TAKEUCHI, Y. (1965) Structures of brittle micas. *Clays Clay Minerals, Proc. 13th Nat. Conf.* **1964,** 1–25.

———, AND R. SADANAGA (1959) The crystal structure of xanthophyllite. *Acta Crystallogr.* **12,** 945–946.

———, AND ——— (1966) Structural studies of brittle micas. (I) The structure of xanthophyllite refined. *Mineral. J.* **4,** 424–437.

TSCHERMAK, G., AND L. SIPÖCZ (1879) Die Clintonitgruppe. *Z. Kristallogr.* **3,** 496–515.

VEITCH, L. G., AND E. W. RADOSLOVICH (1963) The cell dimensions and symmetry of layer-lattice silicates. III. Octahedral ordering. *Am. Mineral.* **48,** 62–75.

VELDE, B. (1973) Détermination expérimentale de la limite de stabilité thermique supérieure des clintonites magnésiennes (abstr.). *Reunion Annu. Sci. Terre, Paris,* **1973,** 409.

YODER, H. S., JR., AND H. P. EUGSTER (1955) Synthetic and natural muscovites. *Geochim. Cosmochim. Acta,* **8,** 225–280.

*Manuscript received, June 4, 1974; accepted for publication, October 31, 1974.*